PHYSICAL REVIEW B VOLUME 51, NUMBER 19 15 MAY 1995-I

Atomic clusters: Building blocks for a class of solids

S. N. Khanna and P. Jena
Physics Department, Virginia Commonwealth University, Richmond, Virginia 23284-2000
(Received 2 June 1994; revised manuscript received 31 October 1994)

Atomic clusters with suitable size and composition can be designed to mimic the chemistry of atoms in the Periodic Table. These clusters which can be viewed as "super atoms" could then form the building blocks for a class of solids with unique structural, electronic, optical, magnetic, and thermodynamic properties. Using density-functional calculations, we outline the design principles for these clusters and describe the role of geometry and electronic shell structure on cluster-cluster interaction.

I. INTRODUCTION

In the last decade, enormous progress has been made in the synthesis, characterization, and fundamental understanding of materials with atomic dimension.[1] This has occurred because of innovations in both experimental and theoretical methods. Using a variety of techniques such as supersonic jet expansion, molecular- and cluster-beam epitaxy, chemical vapor deposition, matrix isolation, scanning tunneling microscope, etc., materials with controlled size and dimension ranging from clusters of a few atoms to nanostructures with thousands of atoms to ultrathin films, with nanometer thickness, can be synthesized. The electronic, magnetic, and optical properties of these mesoscopic systems are unique functions of their size, composition, and topology. Developments of theoretical methods aided by powerful computer codes and high-performance computers have not only made it possible to analyze complex experimental data, but also have enabled one to predict properties that can be verified experimentally. The quantitative accuracy of the predictions is such that current theoretical methods can be used to design materials with tailored properties.

These developments are redefining the frontiers of materials science for the next century. One is now able to design as well as synthesize materials by manipulating individual atoms one by one.[2] These atomically engineered materials include, for example, quantum dots, quantum wells, and quantum corrals. However, most of these investigations focus on using atoms as building blocks of matter. Not much emphasis has been put on synthesizing materials with alternate building blocks, such as clusters. If stable clusters can be synthesized to mimic the chemistry of atoms in the Periodic Table, an additional class of materials with tailored properties could be produced by starting with clusters as building blocks.[3] This phase of materials, best described as cluster materials, can enable researchers to construct a three-dimensional Periodic Table with the size and composition of clusters defining the third dimension. Since, in principle, there is no limit to the size and composition of clusters, the possibilities for additional materials is unlimited. It is not unreasonable to expect cluster-assembled materials to exhibit unique properties. Consider, for example, materials with molecules as building blocks. Water consists of H_2O molecules as building blocks, and its properties are well known. A mixture of hydrogen and oxygen atoms in the same proportion as in the H_2O molecule, however, do not have the same property as water. Unfortunately, the number of molecular materials is rather limited.

Clusters can be thought of as artificial molecules. That crystals of clusters can have properties very different from crystals of the same atoms can be illustrated by comparing the properties of fulleride, diamond, and graphite. Each of these materials is composed of carbon atoms, although fulleride is a crystal of C_{60} clusters,[4] while diamond and graphite are crystals with C atoms as building blocks. The superconducting transition temperature of alkali-doped C_{60} crystal[5] is an order of magnitude higher than that of intercalated graphite. Another cluster that has the potential for forming additional material was recently discovered by Guo, Kerns, and Castleman.[6] It consists of transition metal and carbon atoms with the composition M_8C_{12} and is referred to as metallocarbohedrenes, or met-cars. Unlike C_{60}, which forms a van der Waal's solid, the met-cars are expected to interact with each other more strongly and form a polymeric structure.[7] The presence of transition-metal atoms in the met-car is likely to give a met-car-assembled materials unusual electrical, magnetic, and optical properties[8] that are not seen in C_{60} crystals. Studies of met-car-assembled materials, however, have to wait until bulk quantities of these clusters can be produced. It is important to realize that both C_{60} and met-cars were discovered accidentally. It would be ideal if, by following some fundamental principles, clusters could be designed that have the potential of forming a cluster-assembled material.

These cluster-assembled materials, like molecular crystals, are expected to exhibit unique properties for the following reasons. (1) The electronic band structure of a solid evolves as the atomic energy levels overlap and broaden to form a band. The electron energy levels of a cluster are much more complex than those found in atoms, and are determined not only by the size and composition of the cluster but also by its symmetry. This can be seen from Fig. 1, which compares energy levels of an Al atom with those in an icosahedral Al_{13} cluster. Thus the overlap of cluster energy levels in a cluster solid is likely to be very different from that in a conventional

 ©1995 The American Physical Society

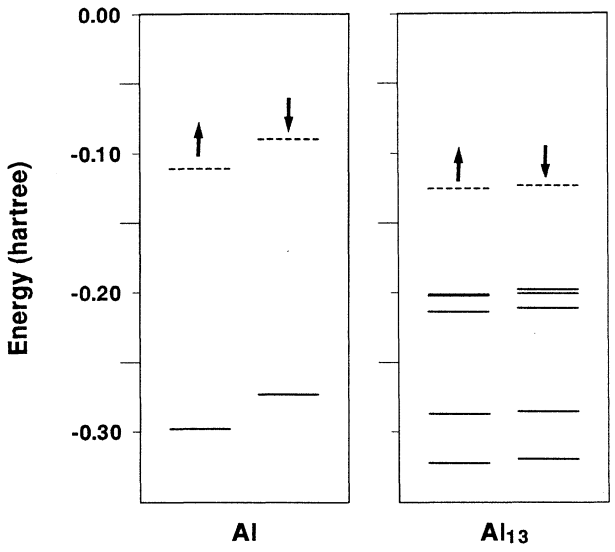

FIG. 1. (a) Energy levels of electrons in an Al atom. (b) Energy levels of electrons in an Al_{13} cluster.

solid. (2) The lattice constant of a cluster-assembled crystal is expected to be large and could also influence the energy-band structure. (3) The phonon spectra of cluster solids are also susceptible to significant changes due to the coupling of intracluster and intercluster vibrations.

In recent years the development of laser vaporization and supersonic jet expansion techniques has enabled researchers to produce and mass select clusters of virtually any atom in the Periodic Table. The size of these clusters can range from a few atoms to a few thousand atoms. By changing the source materials, both homoatomic and heteroatomic clusters can be produced. Since the properties of clusters depend strongly on their size and composition, it is possible to design an unlimited number of clusters that mimic the chemistry of one of the atoms in the Periodic Table. Materials with tailored properties could then be synthesized by assembling these clusters into materials.

One of the disadvantages one could envision of a cluster solid is that it would be in a metastable state, as nature would always follow the path of minimum energy and give rise to atom-assembled materials in the form we know today. This metastability should not be a serious consideration to stand in the way of developing cluster-assembled materials, since we know that crystals of C_{60} clusters, although metastable, can exist for a long time. To make cluster-assembled materials, one simply has to change the synthesis technique, whereby the atoms would first be allowed to form clusters of a certain size and then be allowed to interact to form the metastable material.

In practice, however, there are serious problems in synthesizing cluster-assembled materials in bulk quantities: (1) There are no efficient methods for producing mass-selected clusters in large quantities, although recent progress in generating cluster beams[9] is slowly taking us in that direction. (2) Clusters are metastable against further growth. Thus, when clusters are brought together, they tend to coalesce. Their individual properties are lost and the merits for synthesizing cluster-assembled materials disappear. Steps can, however, be taken to prevent clusters from coalescing. Clusters, once produced, can be mass selected and isolated from each other by embedding them in matrices such as zeolites, rare-gas solids, biological systems, or noninteracting substrates.[10] There are nagging problems, however. The properties of clusters, for instance, can be influenced by the embedding matrix.[11] Thus custom design of a cluster-assembled material must take into account the effect of the matrix. It would be ideal if clusters could be designed in such a way that they would retain their structural identity when assembled into a material. To this end, an understanding of various factors that affect cluster stability and reactivity is important.

To gain insight into the design of clusters, it is useful to analyze the electronic structure of metal clusters *vis a vis* atoms. In Fig. 2(a), we plot the ionization potentials of atoms[12] as a function of their atomic number, Z, and compare this trend with that in Na_N clusters[13] in Fig. 2(b). Note that the ionization potentials of atoms are characterized by a dominant feature—sharp peaks at atomic numbers corresponding to rare-gas atoms. The high ionization potential of rare-gas atoms is due to the fact that their outermost s and p orbitals are filled (ns^2np^6), and it costs more energy to excite the electrons to the next unfilled shell. This also gives these atoms their chemical inertness and high stability. The less prominent peaks in the ionization potential correspond to atoms with filled s shells and half-filled p shells. Consequently, elements with filled s shells and/or half-filled p shells are more reactive than the rare-gas atoms. These features disappear when $20<Z<30$. For these elements, filling of the $3d$ orbitals muddies the simple shell closure effects. Comparison of the ionization potentials of atoms with those of Na_N cluster yields some interesting insight. Note that the ionization potentials for Na_N clusters in Fig. 2(b) exhibit sharp peaks at $N=2$ and 8. These clusters also appear abundantly in the mass spectra, and are commonly referred to as magic clusters. For clusters consisting of more than eight atoms, the ionization potentials continue to oscillate. However, the amplitude of the oscillations are within the errors of the experiment and therefore not much physics can be attributed to these oscillations. Comparison of Figs. 2(a) and 2(b) clearly suggests that Na_N clusters with $N=2$ and 8 must have something in common with the noble gas atoms.

The above comparisons lead one to believe that clusters may be thought of as super atoms.[14] In an atom, the positive charge is localized at a point in the nucleus, namely,

$$n_+^{\text{atom}}(\mathbf{r})=Z\delta(\mathbf{r}) , \tag{1}$$

where Z is the atomic number and $\delta(\mathbf{r})$ is the Dirac delta function. In the jellium model of a cluster,[14] one can imagine that the positive charge of the ions are distributed over the size of the cluster, namely,

$$n_+^{\text{cluster}}(\mathbf{r})=n_0\Theta(\mathbf{R}-\mathbf{r}) , \tag{2}$$

where n_0 is the homogeneous density of positive ions and is given by $n_0 = Z_v/\Omega_0$. Z_v is the valence charge, Ω_0 is the atomic volume, and Θ is the step function. The radius R of this jellium cluster is related to the number of atoms, N, by

$$\frac{4\pi}{3}R^3 = N\Omega_0 \ . \tag{3}$$

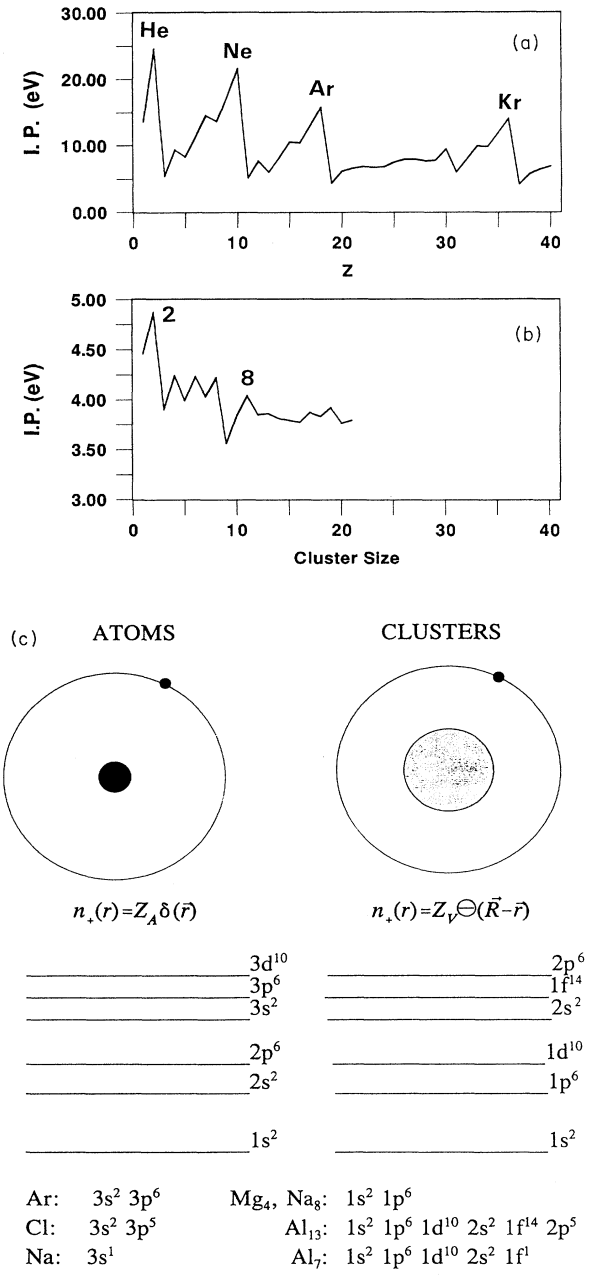

FIG. 2. (a) The ionization potential of atoms as a function of atomic number. (b) The ionization potential of Na_n clusters as a function of cluster size. (c) Comparison of energy levels in an atom and a superatom (cluster).

The difference between an atom and a super atom (cluster) is due to the extent of localization of the positive charge. In an atom, the positive charge is localized at the nucleus. In a jellium model of a cluster, the charge is smeared over the entire cluster. The potential that the electrons see due to the positive charges in both cases are spherically symmetric and the orbital angular momentum l is a good quantum number. The electrons fill the nl orbitals in keeping with the Pauli exclusion principle, although, due to the nature of charge distribution in Eqs. (1) and (3), the ordering of the nl levels are different. In atoms, the nl levels correspond to $1s^2 2s^2 2p^6 3s^2 3p^6 \ldots$, while in clusters they correspond to $1s^2 1p^6 1d^{10} 2s^2 1f^{14} 2p^6 \ldots$ [see Fig. 2(c)]. Thus the electronic shell structures of clusters with 2,8,20,. . . electrons are characterized by $1s^2$, $1s^2 1p^6$, and $1s^2 1p^6 1d^{10} 2s^2 \ldots$, shells respectively. These magic clusters, like the inert gas atoms, have closed electronic shells. The shells closures contribute to their unusual stability, as well as to their high ionization thresholds.

The magic number clusters are also chemically inert, as are the rare-gas atoms. This was demonstrated by Leuchtner, Harms, and Castleman,[15] who studied the reaction of Al_{13} clusters with oxygen. They observed that while Al_{13} reacted strongly, Al_{13}^- was chemically inert. This can be directly attributed to the electronic shell structure. The Al_{13} cluster has 39 electrons, one short of completing the outermost $2p$ shell, whereas Al_{13}^- represents a closed-shell configuration ($1s^2 1p^6 1d^{10} 2s^2 1f^{14} 2p^6$).

The above properties of magic clusters imply that they may be assembled into a material form without the risk of their coalescing into larger clusters. It is not necessary that only monovalent atoms should be used to form magic clusters. One can design a compound cluster in such a way that the total number of valence electrons equals one of the magic numbers, N_c:

$$N_c = \sum_i X^i Z_v^i \ . \tag{4}$$

Here X^i is the number of metal atoms with Z_v^i valence electrons. The summation over i represents the types of different atoms that make up a cluster. The variations in X^i and Z_v^i can yield a large number of magic clusters.

In this paper, we focus on the design of clusters that are likely to keep their structure intact when assembled in a bulk form. We treat these clusters as super atoms and show that, by changing their size and composition, one can create not only chemically inert but also reactive clusters that mimic the properties of rare gas as well as reactive atoms. Using the self-consistent molecular-orbital theory and density-functional method, we have calculated the energetics and electronic structure of a number of clusters with varying size and composition. We have also analyzed, separately, the effect of geometry and electronic shell structure on cluster reactivity. This understanding can lead us to design clusters suitable for forming cluster materials. The paper is organized as follows.

In Sec. II we briefly outline our theoretical procedure.

The effect of geometry and electronic shell structure on cluster reactivity is studied in detail in Sec. III. The electronic structure of clusters and their assemblies are discussed in Sec. IV. The conclusions are summarized in Sec. V.

II. THEORY

The theoretical calculations were carried out using a linear combination of atomic orbitals—molecular-orbital (LCAO-MO) approach. The molecular orbitals were expanded in Gaussian basis functions centered at the atomic sites. Further, the core effects were incorporated through nonlocal norm-conserving pseudopotentials,[16] and the exchange-correlation effects were included via the local-density approximation. In this work, we have used the form of the exchange-correlation functional[17] proposed by Ceperley and Alder and parametrized by Perdew and Zunger.

The use of pseudopotentials instead of all electrons requires the generation of Gaussian basis sets appropriate to pseudo-orbitals. To generate these, the pseudoatom Kohn-Sham equation[18] was numerically solved on a radial mesh of points. The numerical pseudo-orbitals were then fitted nonlinearly to a set of Gaussians. The resulting basis sets were entirely uncontracted and were tested by their ability to reproduce one-electron levels, as well as atomic energy based on the numerical program. They were further tested by calculating the first and second ionization potentials and comparing them with those obtained from the numerical program. The basis sets used in this work consisted of $5s$ and $4p$ Gaussians for C and Al, $4s$ and $2p$ Gaussians for Mg, and $4s$ and $3p$ Gaussians for K. The exponents of the Gaussian basis sets are given in Table I.

TABLE I. Exponents (a.u.) of the Gaussian basis sets employed in this work.

Element	s	p
Mg	1.229 900	0.120 692
	0.829 423	0.032 466
	0.118 557	
	0.043 026	
C	7.554 730	4.946 190
	2.700 760	1.381 860
	0.965 499	0.386 064
	0.345 158	0.107 858
	0.123 391	
Al	2.040 820	0.787 821
	0.853 735	0.257 422
	0.357 143	0.089 965
	0.149 404	0.031 891
	0.062 500	
K	0.197 700	0.045 000
	0.091 357	0.015 000
	0.031 926	0.008 000
	0.013 521	

The electronic structure of the cluster was determined by solving the Kohn-Sham equation[19]

$$(-1/2\nabla^2+V_{\rm ion}+V_H+V_{\rm xc})|\psi_i^\sigma\rangle=E_{i\sigma}|\psi_i^\sigma\rangle \tag{5}$$

self-consistently. Here $V_{\rm ion}$ is the ionic pseudopotential, V_H is the Hartree potential, and $V_{\rm xc}$ is the exchange-correlation potential. $|\psi_i^\sigma\rangle$ is the molecular orbital expanded in terms of the Gaussian basis as

$$|\psi_i^\sigma\rangle=\sum_j C_{ij}^\sigma|g_j\rangle\ . \tag{6}$$

Here σ is the spin index, and C_{ij}^σ are the coefficients to be determined via a self-consistent solution of Eq. (5). The matrix elements of the Hartree and exchange-correlation potential required to solve Eq. (5) were obtained by expanding these potentials in a set of Gaussians centered at the atomic sites and in between the bonds. The total energy was calculated using the local-density expression

$$\begin{aligned}E=&\sum_{i,\sigma}\langle\psi_i^\sigma|-\tfrac{1}{2}\nabla^2+V_{\rm ion}|\psi_i^\sigma\rangle\\&+\tfrac{1}{2}\int\int\frac{\rho(\mathbf{r})\rho(\mathbf{r}')}{|\mathbf{r}'-\mathbf{r}|}d^3r\,d^3r'+\int\epsilon_{\rm xc}(\mathbf{r})\rho(\mathbf{r})d^3r\\&+\tfrac{1}{2}\sum_{\substack{i,j\\i\neq j}}\frac{Z_iZ_j}{|\mathbf{R}_i-\mathbf{R}_j|}\ .\end{aligned} \tag{7}$$

Here $\rho(\mathbf{r})$ is the charge density at the point $\mathbf{r}$, $\epsilon_{\rm xc}$ is the exchange-correlation energy, and Z_i is the charge on the ith ion located at R_i. For details, the reader is referred to earlier papers.[19]

The ground-state geometries require energy minimization with respect to all geometrical distortions. For small clusters, the number of possible parameters is small, and the geometries were optimized by starting from several random initial configurations. For larger clusters, however, only symmetric distortions were allowed. These will be outlined as they appear in the text.

By comparing the energetics of interaction between a Mg atom and a Mg_4 cluster with that between two Mg_4 clusters, the effect of electron shell closure on cluster reactivity can be illustrated. Note that a Mg atom is characterized by the s-shell closure, whereas a Mg_4 cluster is characterized by sp-shell closure. The effect of geometry and composition on cluster-cluster interaction is illustrated by comparing the energetics of two interacting Mg_4:Mg_4 and Al_2Mg:Al_2Mg clusters. Each of these clusters has eight electrons, but different geometry and composition. Mg_4 is a tetrahedron, while Al_2Mg is triangular. The effect of electronic structure on cluster-cluster interaction can be further studied by comparing the energetics between interacting Al_3:Al_3 and Al_2Mg:Al_2Mg. The equilibrium geometries of both Al_3 and Al_2Mg are triangular, but Al_3 has nine electrons, while Al_2Mg has eight electrons. On the other hand, an $(Al_3)_2$ cluster has 18 electrons and corresponds to the magic series, while Al_3 does not. The interaction between Al_3:Al_3 and Al_2Mg:Al_2Mg can be further compared to that between Mg_4:Mg_4 to illustrate the combined effect of geometry and electronic structure on cluster reactivity. In Table II, we list the binding-energy per atom and ion-

TABLE II. Binding energy and ionization potentials of Al_3, Al_2Mg, Mg_4, $(Al_3)_2$, $(Al_2Mg)_2$, and $(Mg_4)_2$ clusters based upon local-spin-density calculations.

Cluster	Binding energy per atom (eV)	Ion. poten. (eV)	Vertical HOMO-LUMO gap (eV)
Al_3	1.45	6.91	0.48
Al_2Mg	0.96	6.04	0.01
Mg_4	0.49	6.61	1.95
$(Al_3)_2$	0.59		0.0
$(Al_2Mg)_2$	0.53		0.46
$(Mg_4)_2$	0.09		0.72

ization potential of the above clusters. It should be pointed out that in all these calculations we have considered only the low-spin configurations, as we are interested in cluster materials.

III. EFFECT OF GEOMETRY AND ELECTRONIC STRUCTURE

A. The role of electronic shell structure

The outermost electronic shell configuration of a Mg atom is $3s^2$, and the interaction between two Mg atoms is characterized by the van der Waal's interaction. However, as Mg atoms are assembled to form a crystal, the strong hybridization[19] between s and p levels gives rise to a Mg metal. The Mg_4 cluster, on the other hand, is characterized by $1s^21p^6$ shell closure and has an atomization energy of 2.00 eV. It is interesting to see if the $1s^21p^6$ shells of Mg_4 clusters would hybridize when they are assembled. Would such a cluster-assembled crystal be metallic? The answer would of course depend upon (a) the Mg_4 clusters retaining their structure after they are assembled to form a crystal, and (b) the degree to which Mg_4 levels hybridize with each other. To answer this, we have carried out detailed studies of total energies and geometrical structure changes, as Mg and Mg_4 were allowed to interact separately with another Mg_4. The geometries of the interacting clusters are given in Figs. 3(a) and 3(b). We first discuss the energetics of a pair of interacting Mg_4 clusters. We allowed each Mg_4 cluster to have three degrees of freedom as they approached each other. For a fixed intercluster distance d between the basal planes shown in Fig. 3(a), the clusters had the freedom to simultaneously rotate about a common axis by an angle θ and readjust the bond lengths r and s. At a given distance d, the optimum values of r, s, and θ were determined by minimizing the total energy of the coupled clusters. In Fig. 4, we present the dependence of r, s, and θ, as well as the binding energy per atom, ΔE, on the intercluster distance d. ΔE is defined by

$$\Delta E=[E(\mathrm{Mg}_n{:}\mathrm{Mg}_m)-E(\mathrm{Mg}_n)-E(\mathrm{Mg}_m)]/(n+m)\ , \tag{8}$$

where $E(\mathrm{Mg}_n{:}\mathrm{Mg}_m)$ is the total energy of the two interacting Mg_n and Mg_m clusters at their optimized configuration, $n+m$ is the total number of atoms, and $E(\mathrm{Mg}_n)$ is the energy of an isolated Mg_n cluster. Note that the variation in the geometrical parameters r, s, and θ are minimal for $d \gtrsim 6a_0$. The energy of the interacting clusters reaches a minimum when $d \simeq 5.8a_0$. At this point, θ abruptly changes to 60°, while the variation in r and s still remains small. This rotation of the Mg_4 cluster occurs because of the repulsion between the Mg atoms at short distances. The structure of the individual clusters become unstable only when further energy is supplied to push the clusters to closer proximity. The binding energy per atom in Eq. (8) of the $(Mg_4)_2$ cluster is 0.1 eV. This is

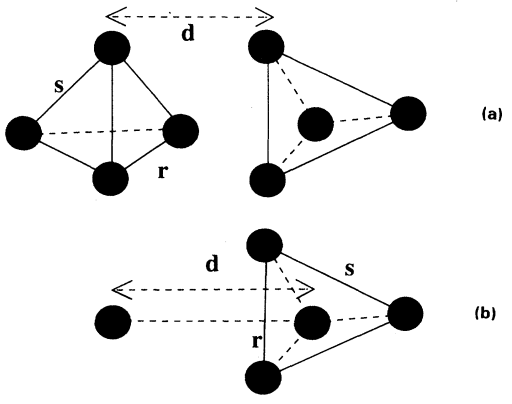

FIG. 3. Geometries of interacting (a) Mg_4:Mg_4 and Mg_4:Mg clusters. d is the distance between the basel planes of the tetrahedras.

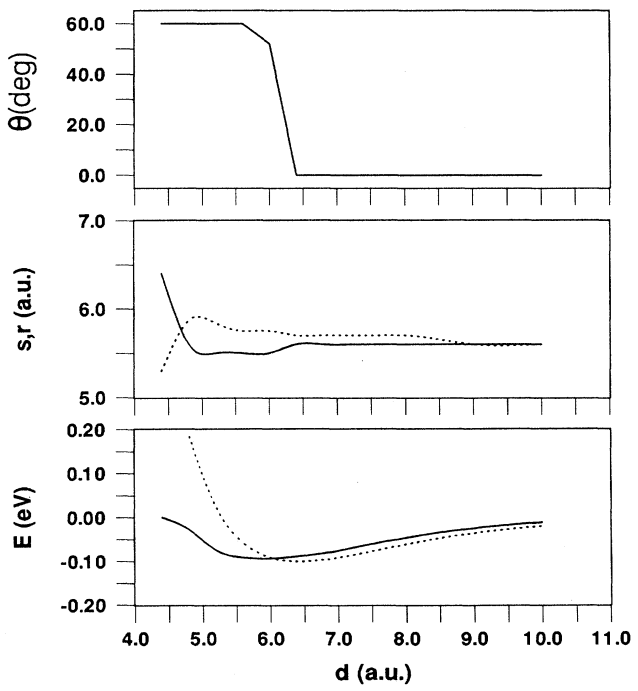

FIG. 4. The dependence of binding energy and cluster parameters r, s, and θ on intercluster distance in Mg_4:Mg_4 interacting clusters. The dotted line in the energy curve corresponds to the interaction energy in the Mg_2 molecule.

very close to the binding energy of the Mg_2 dimer, which is also 0.1 eV. Since the Mg_2 interaction is known to be of the van der Waal's type, one can conclude that Mg_4-Mg_4 interacts via a van der Waal's mechanism. This is what one could have expected since the Mg_4 cluster, with its eight electrons, has a closed electronic shell and therefore is chemically inert. Can Mg_4 clusters be assembled to form a new Mg crystal? This would depend upon how strongly the Mg_4 energy levels overlap when they are assembled to form a crystal. Recall that bulk Mg becomes metallic even if the Mg_2 dimer is van der Waal bonded. Insight into this problem can be gained by studying the interaction of a Mg atom with a Mg_4 cluster. Is a Mg atom more reactive than a Mg_4 cluster?

The interaction between a Mg atom and Mg_4 cluster was studied by calculating the binding energy and changes in the Mg_4 cluster geometry as a Mg atom was brought toward a Mg_4 cluster [see Fig. 3(b)]. In Fig. 5, we plot the energetics of interacting Mg_4-Mg clusters. We note that the binding energy per atom of a Mg-Mg_4 coupled cluster is also 0.1 eV, which is similar to that in $(Mg_4)_2$, as well as to that in a Mg_2 dimer. However, the structural distortion of the Mg_4 cluster as a Mg atom is brought in is somewhat larger than that in Fig. 4. This indicates that the interaction between two closed-shell clusters does depend, however weakly, on which shells are closed. This is consistent with the chemistry of atoms. An atom with a closed *s* shell is more reactive than one with closed *sp* shells. This aspect is reflected in the ionization potential, as discussed above in Fig. 1(a).

To understand why an Mg atom can disturb the geometry of a Mg_4 cluster more than another Mg_4 can, we have examined the energy level structures of Mg and Mg_4 clusters. We note that the HOMO-LUMO [highest (lowest) occupied (unoccupied) molecular orbital] gap and the ionization potential of the Mg atom are 3.3 and 7.6 eV, respectively, while in Mg_4 clusters these are 1.9 and 6.6 eV, respectively. Thus if the HOMO-LUMO gap and the ionization potential were the only deciding factors, a Mg atom should be more inert than a Mg_4 cluster. An equally important factor that governs cluster reactivity is also influenced by the degree to which the energy levels of interacting species hybridize as they approach each other. The considerable hybridization between *s* and *p* states as Mg atoms come together results from a strong splitting of the bonding and antibonding states. In the case of a Mg_4 cluster, the LUMO orbital is of *d* type and is narrow. The splitting of these narrow orbitals as Mg_4 clusters approach each other is small, thus reducing the changes for overlap. To form cluster assemblies, it may be preferable to start with clusters that have closed *sp* shells.

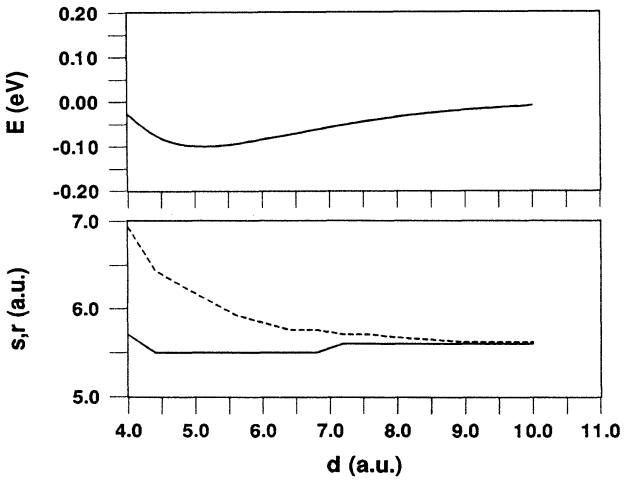

FIG. 5. The dependence of binding energy and cluster parameters *r* and *s* on intercluster distance in Mg_4:Mg interacting clusters.

B. The role of geometry

In Sec. II A, we demonstrated that the reaction of a cluster can be influenced by its electronic shell structure. Here we examine the role of geometry on cluster reactivity by comparing the interaction between two different sets of clusters with similar electronic but different atomic structures. Consider, for example, Mg_4 and Al_2Mg clusters. Both clusters have eight valence electrons. However, Mg_4 is a perfect tetrahedron, while Al_2Mg can at best form a two-dimensional structure—far from being spherical. In addition, Al_2Mg is composed of two different kinds of atoms. Thus a comparison between the binding energies and change of geometrical parameters as a function of intercluster distance for interacting Mg_4-Mg_4 and Al_2Mg:Al_2Mg clusters would illustrate the role of geometry and composition on cluster reactivity.

We found the equilibrium geometry of a single Al_2Mg cluster to be triangular. The corresponding geometrical parameters and its atomization energy are given in Table II. The two Al_2Mg clusters were brought together with the Al-Al bonds perpendicular to each other (see Fig. 6). At each distance *d*, we optimized the Al-Al distance *s* and Al-Mg distance *r*. The binding energy per atom of $(Al_2Mg)_2$, as a function of *d*, $\Delta E = [E(Al_2Mg{:}Al_2Mg) - 2E(Al_2Mg)]/6$, is plotted in Fig. 7. Note that for

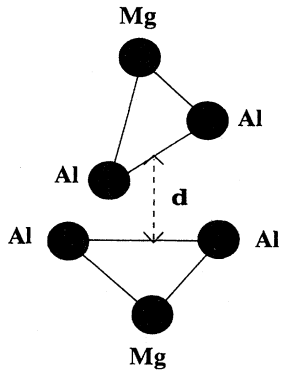

FIG. 6. Geometry of interacting Al_2Mg clusters. The planes of the two clusters are perpendicular to each other.

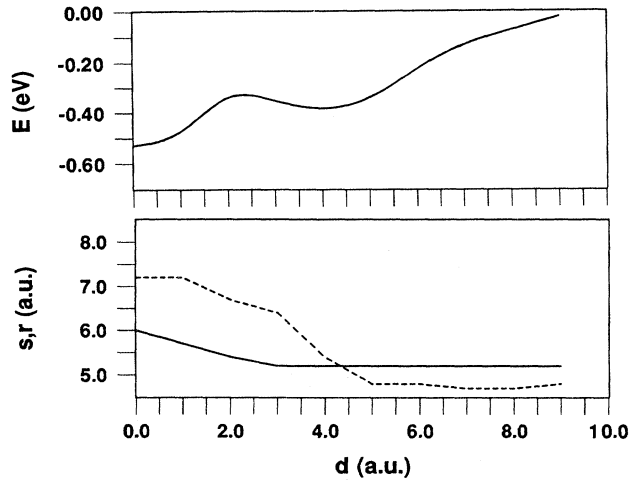

FIG. 7. Binding energies of two interacting Al_2Mg clusters and geometrical parameters as a function of intercluster distance.

$d > 4a_0$, there are minimal changes in the geometry of the individual Al_2Mg clusters. At shorter distances, the interaction between the Al atoms increases rapidly, and the geometry of the $(Al_2Mg)_2$ undergoes significant modification. The binding energy per atom of $(Al_2Mg)_2$ is nearly 0.5 eV. These results should be compared with the interacting Mg_4-Mg_4 clusters in Fig. 4. Recall that the binding energy of $(Mg_4)_2$ is only 0.1 eV/atom, and the geometry of Mg_4 remains practically unchanged. Thus, even though both Al_2Mg and Mg_4 have eight valence electrons, their mutual interactions are quite different. It is clear that the geometry and composition of a cluster has a significant role to play on the chemistry of a cluster.

The different reactivities of Al_2Mg and Mg_4 clusters can be understood by comparing their electron energy levels (see Fig. 8). Note that Mg_4 is characterized by a HOMO-LUMO gap of nearly 2 eV, while the corresponding gap in Al_2Mg is practically zero. This is caused not only because the electron energy levels of Mg and Al atoms are different (see Fig. 8), but also the planar geometry of the Al_2Mg cluster leads to a larger rearrangement of energy levels due to the Jahn-Teller effect.

C. The role of electronic structure

The role of electronic structure alone can be illustrated by comparing the energetics of interaction between two Al_3 clusters with that of the two Al_2Mg clusters discussed above. Note that while both Al_2Mg and Al_3 have triangular geometries, they have a different number of valence electrons. In Fig. 9, we plot the binding energy per atom, $\Delta E = [E(Al_3{:}Al_3) - 2E(Al_3)]/6$, of two interacting Al_3 clusters as a function of intercluster distance d. The two Al_3 cluster are brought toward each other in the same manner as that shown in Fig. 6. As in the case of $Al_2Mg{:}Al_2Mg$ interaction, we also optimized the bond lengths r and s at each distance d of the interacting $Al_3{:}Al_3$ clusters. The variation of these parameters is also plotted in Fig. 9. Note that there are two minima in the binding energy as the Al_3 clusters approach each other. One of the minima corresponds to a configuration where the central four atoms lie on a plane, while the other minima arises when the two sets of atoms are at a distance. Both states are nearly degenerate, and the equilibrium geometry given earlier by Upton[20] corresponds to the first configuration discussed above. The parameters listed in Table II correspond to the first configuration. The binding energy of $(Al_3)_2$ is about 0.6 eV/atom, and is comparable to the 0.5 eV/atom found in $(Al_2Mg)_2$. The geometries of Al_3 clusters also undergo changes similar to those found in Fig. 7. We further note from Fig. 8 that the energy levels of Al_3 clusters are not too different from those of Al_2Mg. This clearly indicates that the geometry of a cluster is indeed an important factor in cluster reactivity.

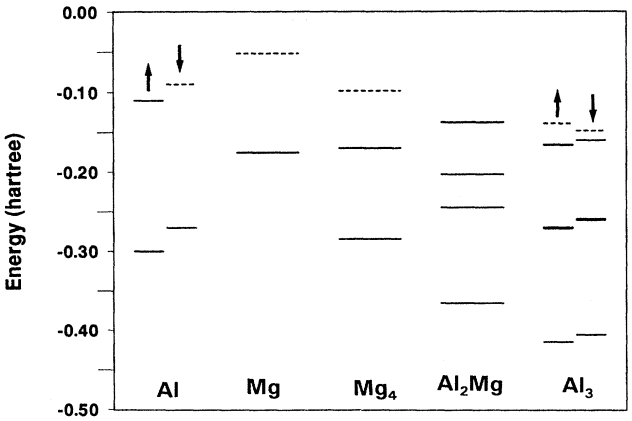

FIG. 8. Energy levels of Al, Mg, Mg_4, Al_2Mg, and Al_3 clusters.

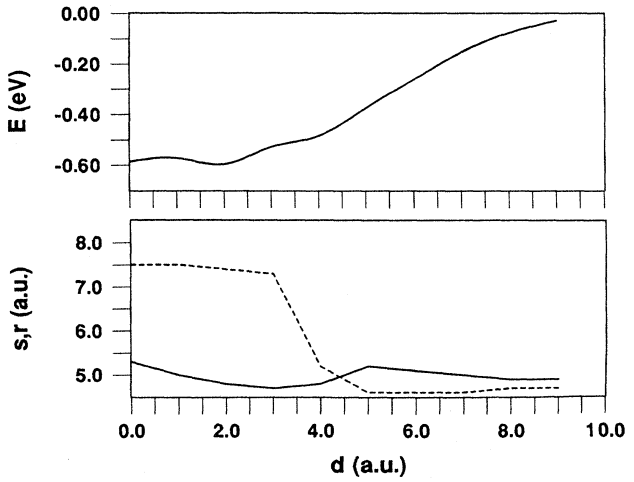

FIG. 9. Binding energies of two interacting Al_3 clusters and geometrical parameters as a function of intercluster distance.

IV. DESIGN OF STABLE CLUSTERS

From the above discussion, it is clear that both the electronic shell structure and geometrical structure of clusters should be taken into account while designing chemically inert clusters. We should point out, at this stage, that the importance of atomic structure of clusters, with regard to their stability, was noted by Martin *et al.*[21] in an experiment involving Cs clusters. They found that while the enhanced stability of small clusters was dominated by the electronic shell structure, the atomic shell structure was important for the relative stability of large clusters. Thus, in designing clusters to form cluster materials, it is important to pay attention to both geometry and electronic structure. In the following, we discuss the design of two different kinds of clusters suitable for assembling into a material.

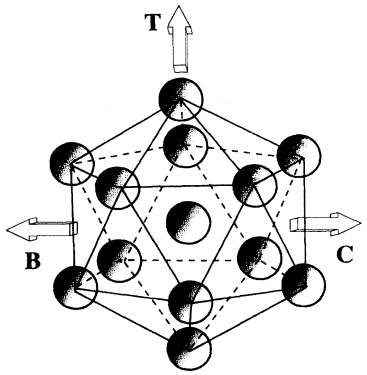

FIG. 10. Icosahedric structure of the Al_{13} cluster. Also shown are the on-top (T), bridge (B), and hollow (C) directions.

A. Weakly bonded clusters

We first discuss the design of very stable and chemically inert clusters. We begin with the Al_{13} cluster as an example, and demonstrate how it can be modified to satisfy the design criteria. It has been shown earlier[22] that the preferred atomic structure of the Al_{13} is an icosahedron (Fig. 10), which is the most compact structure the 13-atom cluster can have. Using the method described in Sec. II, we have calculated the atomic structure, binding energy, and electronic properties of the Al_{13} cluster, and have compared these to previous calculations[22,23] in Table III. The agreement between various theoretical results is satisfactory considering that they correspond to various levels of the approximation. While the Al_{13} satisfies the compact geometry requirement, it has 39 electrons, one short of closing the outermost shell. Consequently, it is reactive.

The icosahedric Al_{13} cluster could be made more stable, as well as chemically inert, by suitably doping a tetravalent impurity atom such as C. The compound clusters $Al_{12}C$ have 40 electrons—just enough to close the last electronic shell. To locate possible sites for the impurity atom, it is instructive to compare the binding energies of Al_2 and AlC dimers. In Table IV, we compare our calculated binding energies and bond lengths of these dimers with experiment and previous calculations. The agreement with experiment,[24] as well as the previous *ab initio* result,[25] is very good. Note that the calculated binding energy of AlC is larger than the Al_2 binding energy. (It is likely that the experimental binding energy of AlC may need revision.) Thus it is expected that the impurity atom C would tend toward a site where it can be coordinated to the maximum number of Al atoms. We have, therefore, reoptimized the bond length of $Al_{12}C$ by placing the impurity atom at the center of the icosahedron. Similar calculations were also carried out for $Al_{12}Si$. The resulting bond lengths and binding energies are given in Table V. Both $Al_{12}C$ and $Al_{12}Si$ clusters are more strongly bound than the Al_{13} cluster. $Al_{12}C$ is the most stable cluster, with a binding energy that is 4.4 eV higher than that of Al_{13}. These magic clusters are also characterized by a large HOMO-LUMO gap and ionization potential.

To study the relative reactivity of these clusters, we have calculated[26] the binding energies of a hydrogen atom brought toward the Al_{13} and $Al_{12}C$ clusters along various directions (on top, hollow, and bridge). For each hydrogen distance, the icosahedric bond distance was op-

TABLE III. Comparison of our calculated nearest-neighbor distance, binding energy, and the ionization potential of the Al_{13} cluster with previous results. The nearest-neighbor distance and cohesive energy of bulk Al are 5.40 a.u. and 3.39 eV, respectively.

Authors	Method	Nearest-neighbor distance (a.u.)	Binding energy/atom (eV)	Ionization potential (eV)
Present	Gaussian-LSD	5.07	2.82	7.2
Cheng, Berry, and Whetten	DVM-X	5.25	2.80	6.0
Yi *et al.*	CP-LD		2.97	7.15
Gong and Kumar	DVM-LD	5.32	2.77	7.10
Seitsonen *et al.*	CP-LSD	4.95	3.21	
Dunlap	Gaussian-LSD	5.02	3.04	

TABLE IV. Comparison of our calculated binding energy per atom and bond lengths of Al_2, AlC, and AlK dimers with experimental and previous theoretical values.

Cluster	Present	Ref. 24	Experiment
Al_2 bond length (a.u.)	4.75	5.12	4.84
binding energy (eV)	0.90	0.63	0.78
AlC bond length (a.u.)	3.74	3.78	3.68
binding energy	2.00	1.60	0.93
AlK bond length (a.u.)	7.38		
binding energy (eV)	0.57		

timized. The binding energies of H and its distance from the nearest Al in Al_{13} and $Al_{12}C$ clusters are listed in Table VI. We note that the preferred sites, among those studied for H interacting with $Al_{12}C$ and Al_{13} clusters, are the on-top site and the bridge site, respectively. In addition, the binding energy of H bonded to Al_{13} is 3.24 eV. This is significantly larger than the binding energy of 2.17 eV when H is bonded to $Al_{12}C$. These binding energies should be compared with the binding energy per atom of the H_2 molecule, which in our local-density-functional calculation is 2.4 eV. Thus, it is energetically favorable for a H_2 molecule to dissociate and bind atomically to the Al_{13} cluster, while such a dissociation on the $Al_{12}C$ cluster is not possible.[27] One could argue that the $Al_{12}C$ cluster will remain inert toward H_2 as a result of its closed electronic shell. This finding is consistent with an earlier experimental result of Leuchtner, Harms, and Castleman,[15] where the authors exposed Al_n and Al_n^- clusters to oxygen. They observed that while the Al_{13} cluster reacted strongly with O_2, Al_{13}^- did not. Note that Al_{13}^-, like $Al_{12}C$, has 40 valence electrons.

Further evidence of the inertness of $Al_{12}C$ has come from recent computer simulation studies by Kawai.[28] Using the Car-Parrinelo quantum molecular-dynamics technique, these authors studied the interaction between two $Al_{12}C$ clusters, as well as between two $Al_{12}Si$ clusters. They found that the structure of $Al_{12}C$ clusters remained uanffected, testifying to its stability and chemical inertness. However, they observed that when two $Al_{12}Si$ clusters were allowed to interact, their individual geometries changed. This result is in agreement with a recent study by Seitsonen *et al.*[23] The reason for $Al_{12}C$ to retain its structure while $Al_{12}Si$ cannot, when allowed to interact, can be traced to their respective binding energies. $Al_{12}C$ is 1.9 eV, more strongly bound than $Al_{12}Si$. Moreover, the cohesive energy of Al metal is 3.19 eV, which is smaller than the binding energy difference between $Al_{12}C$ and Al_{13}. It is thus likely that $Al_{12}C$ clusters can be assembled to form another solid. The interesting question then arises: what would the electronic properties of a crystal assembled from $Al_{12}C$ clusters be like? It is clear that a bulk Al with 8% C impurities would remain metallic. Would a crystal of $Al_{12}C$ clusters be metallic?

TABLE V. Energetics and bond lengths of $Al_{12}C$, $Al_{12}Si$, and Al_{13} clusters.

Cluster	Radial distance of the icos. (a.u.)	Binding energy/atom (eV)
Al_{13}	5.06	2.82
$Al_{12}C$	4.78	3.16
$Al_{12}Si$	5.05	3.02

TABLE VI. Binding energy and preferred site of H interacting with Al_{13} and $Al_{12}C$ clusters.

Cluster	Location of H	Radial distance of the icos. (a.u.)	Distance of H to the nearest atom (a.u.)	Binding energy of H (eV)
$Al_{13}H$	on-top	5.06	2.97	2.67
	bridge	5.06	3.33	3.24
$Al_{12}CH$	on-top	4.78	3.02	2.17
	bridge	4.78	3.44	1.50
	hollow	4.78	3.36	1.46
H_2			1.46	4.85

While no electronic band structure and cohesive energy calculations of crystals with $Al_{12}C$ clusters as building blocks have yet been carried out, a qualitative inference can be drawn from a recent model calculation by Manninen *et al.*[29] Here the authors calculated the energy-level structure of a fcc crystal where each lattice site was occupied by a jellium cluster of radius R. The potential of each of these clusters was given by a square-well form

$$V(\mathbf{r}) = V_0 , \quad r \le R \tag{9a}$$

$$= \infty , \quad r \ge R , \tag{9b}$$

where $V_0 = -\phi - \epsilon_F$, ϕ being the work function of Al, and ϵ_F is the Fermi energy measured from the bottom of the conduction band.

The electron energy levels of the fcc crystal for various values of R and different jellium cluster densities were calculated. For the sake of brevity and completeness, we give the energy-band structure for a fcc cluster material with a lattice constant equal to 11.7 Å. This is designed to simulate a crystal of $Al_{12}C$ clusters. The band structure of this model cluster is shown in Fig. 11. The energy bands are rather narrow with a band gap of 0.5 eV. This suggests that a crystal assembled with $Al_{12}C$ clusters is a semiconductor. It will certainly be interesting to carry out a band-structure calculation in which real icosahedric $Al_{12}C$ clusters are arranged at lattice sites of different crystalline forms. Maximization of the cohesive energy

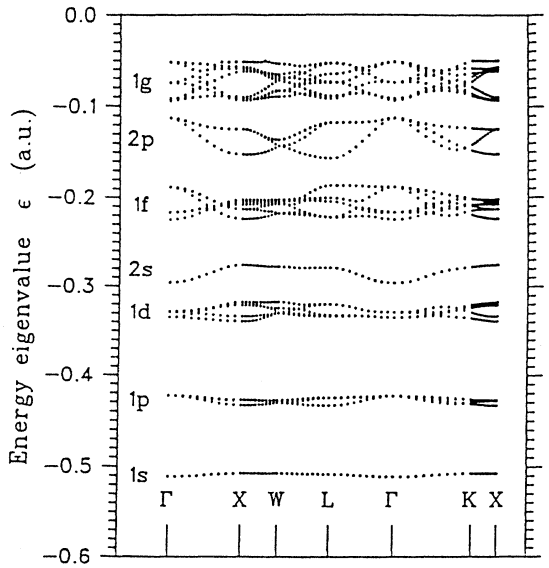

FIG. 11. Band structure of a fcc solid constructed with a cluster modeling $Al_{12}C$ cluster.

can point to the most stable crystal lattice. An experimental investigation of the stability and reactivity of $Al_{12}C$ clusters would also be useful.

Above we discussed assemblies of inert clusters composed of two different kinds of atoms. One could also envision assemblies of inert clusters consisting of only one kind of atom. For example, Mg_4, and K_8 will fall into this category as both clusters have eight electrons each and therefore correspond to magic species. In Sec. II we discussed the interaction of two Mg_4 clusters approaching along a fixed direction. Although the structural component of the clusters remained essentially unchanged, there were significant differences in the HOMO-LUMO gap. In the Mg_4 cluster, the HOMO-LUMO gap is 1.95 eV, while in the $(Mg_4)_2$ cluster the HOMO-LUMO gap reduces to 0.72 eV. This raises an important question. If a crystal of Mg_4 clusters could be produced, would the HOMO-LUMO gap be reduced to zero, and would the corresponding cluster solid become metallic? Recall that the Mg atom is a closed-shell species, but that the Mg crystal is metallic. Second, we have allowed only the Mg_4 clusters to have a specific trajectory for approach. Are there other preferred directions and, if so, would that compromise the structural integrity of the cluster itself? To answer some of these fascinating questions, molecular-dynamics studies of several interacting Mg_4 clusters would be useful. It is hoped that this paper will stimulate such an undertaking.

B. Ionically bonded clusters

In the previous discussion, we demonstrated that clusters can be prevented from coalescing by requiring that they be chemically inert. However, the cohesive energy of solids composed of such weakly interacting clusters would be rather small. Crystals of clusters with larger cohesive energies can be constructed if the clusters interact via ionic, covalent, or metallic bonding. In this section we discuss one such possibility.

Consider a KAl_{13} cluster. It has the same number of valence electrons as $Al_{12}C$, but its geometry is entirely different. We expect the K atom to reside outside the Al_{13} cluster for two reasons. First, the Al_{13} cluster is icosahedric, and there is no room inside the icosahedron to accommodate a large atom such as K. Second, it is not energetically preferable for K to replace any of the Al atoms in the Al_{13} cluster, since the binding energy of KAl dimer is much lower than the binding energy of Al_2 (see Table IV).

To find the location of the K atom, we have calculated[30] the energetics of interaction between the Al_{13} cluster and K by bringing K along three possible directions, as shown in Fig. 10. The binding energies of the KAl_{13} cluster, as a function of distance between K and Al_{13}, along the on-top, hollow, and bridge directions were calculated by optimizing the nearest-neighbor distance between Al atoms in the Al_{13} cluster for each K position. The results of the icosahedric bond lengths and the preferred distance of K from the center of the Al_{13} icosahedron, as well as the binding energy for various configurations of the K atom, are given in Table VII. We note that the binding energy is maximum for K situated along the hollow direction at 9.20 a.u., away from the Al_{13} center. The binding energy of 3.04 eV of K in $Al_{13}K$ is substantially larger than that in the KAl dimer.

This large binding energy between K and Al_{13} is a consequence of a strong ionic bond between K and Al_{13}. This can clearly be seen from the following considerations. The Mulliken charge analysis yields a charge of -1 on Al_{13} and $+1$ on K. Second, the electrostatic attraction between two charges located at distance of 9.20 a.u. (the distance between the center of Al_{13} and K) is 2.96 eV, which is almost identical to the binding energy of 3.04 eV, calculated self-consistently (see Table VII).

The strong ionic bond that stabilizes the KAl_{13} cluster can be understood by noting that the chemistry of the Al_{13} cluster is similar to that of the Cl atom. The electron affinity of the Al_{13} cluster from Table VII is 3.7 eV,

TABLE VII. Geometrical parameters and binding energies of Al_{13}, Al^-_{13}, and $Al_{13}K$ clusters.

Cluster	Bond length (a.u.)	Binding energy/atom (eV)	Distance of K atom (a.u.)
Al_{13}	5.06	2.82	
Al_{13}^-	5.05	3.11	
KAl_{13} (on-top)	5.05	2.42	10.60
KAl_{13} (bridge)	5.05	2.89	9.52
KAl_{13} (hollow)	5.05	3.04	9.20

and is almost identical to the electron affinity of the Cl atom, which is 3.6 eV. Both Al_{13} and Cl have one hole in their outermost electronic shell. The strong ionic bond between KCl arises since K is electropositive while Cl is electronegative. In an analogous way, KAl_{13} also forms a strong ionic bond. One of the major differences between Al_{13} and Cl is that the size of the Al_{13} cluster is about four times larger than the Cl atom. Thus it is expected that a crystal consisting of K and Al_{13} building blocks would possess a large lattice constant.

Unlike in a $Al_{12}C$ crystal, where the individual $Al_{12}C$ clusters are kept apart due to van der Waal's interaction, in a KAl_{13} crystal the Al_{13} clusters will carry a negative charge and can stay away from another Al_{13} cluster due to electrostatic repulsion. The structure of the KAl_{13} crystal would most likely be a body-centered-cubic lattice similar to CsCl (see Fig. 12).

We have estimated the cohesive energy of a bcc KAl_{13} cluster by using the formula[12]

$$U_{\text{tot}}/N = Z\lambda \exp(-R_0/\rho) - \alpha \frac{q^2}{R_0} , \tag{10}$$

where N is the number of ion pairs carrying charge q, Z is the number of nearest neighbors of any ion, and α is the Madelung constant. R_0 is the nearest-neighbor distance. The parameters λ and ρ define the repulsive part of the interaction. For KCl, the repulsive part of the interaction is only 10% of the cohesive energy. In a bcc crystal of $Al_{13}K$, a nearest-neighbor distance of 9.20 a.u. will keep the nearest Al atoms at a distance of 5.06 a.u. This is nearly equal to the nearest-neighbor distance in bulk Al. With this lattice constant, Eq. (10) yields the cohesive energy of KAl_{13} to be 5.2 eV. This is indeed large.

There are several astonishing aspects of the above results. Previous studies[31] have shown that K is immiscible with Al and, in the molten state, only 0.05% of K can be dissolved in Al. In other words, the phase diagram of K_xAl_{1-x} does not yield a KAl_{13} phase. This result is understandable since the KAl bond, as discussed, is much weaker than the Al-Al bond. Thus it is energetically unfavorable for K to occupy a substitutional site. However, if the synthesis technique is modified from assembling crystals from atoms to crystals from clusters of KAl_{13}, an additional crystal phase is possible. The bonding, as outlined above, will be strong due to the ionic nature of K and Al_{13}.

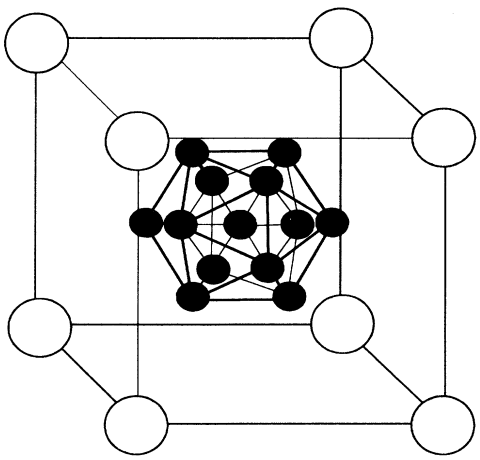

FIG. 12. bcc crystal structure of KAl_{13}.

V. CONCLUSIONS

This paper has focused on the possibility that atomic clusters of suitable size and composition can be designed in such a way that they can retain their geometry, even after they are allowed to interact with each other. Such clusters can then form building blocks for an additional class of materials. It is expected that the properties of these cluster-assembled materials can be very different from other materials that have atoms as building blocks. The variations in cluster size, composition, and geometry can then give rise to a generation of cluster materials with tailored properties.

Using the density-functional theory and molecular-orbital method, we have studied the role of geometry, electronic structure, and symmetry on cluster stability and reactivity. The binding energy and changes in cluster geometry were calculated by allowing various clusters to interact with each other. We have found that electron shell filling, as well as geometrical packing, do influence the stability of clusters. The reactivity of clusters are influenced to a varying degree by the binding energy, HOMO-LUMO gap, ionization potential, and electronic and atomic structure. It is important to consider all these factors in designing clusters suitable for synthesizing cluster materials.

Weakly interacting clusters can be designed by requiring that the total number of valence electrons equal one of the magic numbers of the jellium clusters. This can be achieved by suitably changing the number and type of atoms forming the cluster. We have demonstrated that clusters such as $Al_{12}C$ can exhibit unusual stability due to their compact icosahedric structure and electron shell closure. These clusters interact very weakly with each other and can form the basis for synthesizing material with $A_{12}C$ clusters as building blocks. It is expected that a crystal of $Al_{12}C$ units arranged in a fcc lattice structure would be a semiconductor.

More strongly bound cluster solids can also be synthesized where the clusters are so designed that they stay away from each other due to electrostatic repulsion. As an example, we studied the electronic structure and stability of $Al_{13}K$ cluster. The binding energy of K to Al_{13} was found to be 3.04 eV. This is surprising because K is immiscible in bulk Al, and the binding energy of AlK dimer is rather small compared to the binding energy of Al_2. The unusual binding energy of $Al_{13}K$ is due to the fact that this bonding is characterized by an ionic interaction. Al_{13} is electronegative, while K is electropositive. In the $Al_{13}K$ cluster, Al_{13} exists as an Al_{13}^- and K exists as a K^+ ion. In this sense, the chemistry of Al_{13}

strongly resembles that of a Cl atom. It is argued that a bcc crystal of $Al_{13}K$ may exist with a cohesive energy per pair of nearly 5 eV. This indeed would be remarkable since the cohesive energy of neither bulk Al nor K is this high, and K is immiscible in Al. It will be interesting to see what electrical and optical properties a crystal of $Al_{13}K$ may have.

It is expected that clusters whose properties may mimic those of atoms in the Periodic Table may provide a third dimension to the Periodic Table with the size and composition defining the third dimension. It will be highly rewarding if some of the clusters such as $Al_{12}C$ and $Al_{13}K$ can be synthesized in large enough quantities to form cluster materials. The properties of cluster-assembled materials will certainly give a new dimension to materials science in years to come.

ACKNOWLEDGMENT

This work was funded by a grant from the Department of Energy (DE-FG05-87ER45316).

[1] *Physics and Chemistry of Finite Systems: From Clusters to Crystals,* edited by P. Jena, S. N. Khanna, and B. K. Rao (Kluwer Academic, Dordrecht, The Netherlands, 1992); Proceedings of the Sixth International Conference of Small Particles and Inorganic Clusters [Z. Phys. D **26** (1993)]; *Clusters and Cluster-Assembled Materials,* edited by R. S. Averback, J. Bernholc, and D. L. Nelson, MRS Symposia Proceedings No. 206 (Materials Research Society, Pittsburgh, 1991).

[2] M. G. Lagally, Phys. Today **44** (11), 24 (1993); Science **254**, 1302 (1991).

[3] S. N. Khanna and P. Jena, Phys. Rev. Lett. **69**, 1664 (1992).

[4] W. Kratschmer, L. D. Lamb, K. Fostiropoulos, and D. R. Huffman, Nature (London) **347**, 354 (1990); H. W. Kroto, J. R. Heath, S. C. O'Brien, R. F. Curl, and R. E. Smalley, *ibid.* **318**, 162 (1985).

[5] A. F. Hebard, M. J. Rosseinsky, R. C. Haddon, D. W. Murphy, S. H. Glarum, T. T. M. Palstra, A. P. Ramirez, and A. R. Kortan, Nature **350**, 600 (1991).

[6] B. C. Guo, K. P. Kerns, and A. W. Castleman, Jr., Science **255**, 1411 (1992).

[7] S. Wei, B. C. Guo, J. Purnell, S. Buzza, and A. W. Castleman, Jr., Science **256**, 818 (1992).

[8] B. V. Reddy, S. N. Khanna, and P. Jena, Science **258**, 1640 (1992); B. V. Reddy and S. N. Khanna, Chem. Phys. Lett. **209**, 104 (1993).

[9] O. F. Hagena and G. Knop, in *Physics and Chemistry of Finite Systems: From Clusters to Crystals* (Ref. 1), p. 1233.

[10] T. Castro, R. Reifenberger, E. Choi, and R. P. Andres, Phys. Rev. B **42**, 8548 (1990).

[11] Y. Nozue, T. Kodaira, and T. Goto, Phys. Rev. Lett. **68**, 3789 (1992).

[12] *Introduction to Solid State Physics,* edited by C. Kittel (Wiley, New York, 1986), p. 59.

[13] M. M. Kappes, M. Schar, U. Rothlisberger, C. Yeretzian, and E. Schumacher, Chem. Phys. Lett. **143**, 251 (1988).

[14] W. D. Knight, K. Clementer, W. A. de Heer, W. A. Saunders, M. Y. Chou, and M. L. Cohen, Phys. Rev. Lett. **52**, 2141 (1984); S. Saito and S. Ohnishi, *ibid.* **59**, 190 (1980).

[15] R. E. Leuchtner, A. C. Harms, and A. W. Castleman, Jr., J. Chem. Phys. **91**, 2753 (1989); A. Nakajima, T. Kishi, T. Sugioka, and K. Kaya, Chem. Phys. Lett. **187**, 239 (1991).

[16] G. B. Bachelet, D. R. Hamann, and M. Schluter, Phys. Rev. B **26**, 4199 (1982).

[17] D. M. Ceperley and B. J. Alder, Phys. Rev. Lett. **45**, 566 (1980); J. P. Perdew and A. Zunger, Phys. Rev. B **23**, 5048 (1981).

[18] P. Hohenberg and W. Kohn, Phys. Rev. **136**, B864 (1964); W. Kohn and L. J. Sham, *ibid.* **140**, A1133 (1965).

[19] F. Reuse, S. N. Khanna, V. de Coulon, and X. Buttet, Phys. Rev. B **41**, 11 743 (1990).

[20] T. H. Upton, Phys. Rev. Lett. **56**, 2168 (1986).

[21] T. P. Martin, T. Bergmann, H. Gohlich, and T. Lange, Chem. Phys. Lett. **172**, 209 (1990).

[22] H. P. Cheng, R. S. Berry, and R. L. Whetten, Phys. Rev. B **43**, 10 647 (1991); J. Y. Yi, D. J. Oh, J. Bernholc, and R. Car, Chem. Phys. Lett. **174**, 461 (1990); X. G. Gong and V. Kumar, Phys. Rev. Lett. **70**, 2078 (1993); B. I. Dunlap (private communication).

[23] A. P. Seitsonen, M. J. Puska, M. Alatalo, R. M. Nieminen, V. Milman, and M. C. Payne, Phys. Rev. B **48**, 1981 (1993).

[24] V. I. Vedeneyeu, L. V. Gurvich, V. N. Kondratyeu, V. A. Madvedeu, and Y. L. Frankevich, *Bond Energies, Ionization Potentials and Electron Affinities* (St. Martin's, New York, 1966), p. 31.

[25] B. K. Rao and P. Jena, Appl. Phys. Lett. **57**, 2308 (1990).

[26] S. N. Khanna and P. Jena, Chem. Phys. Lett. **218**, 383 (1994).

[27] We have not studied the binding energy of H to the threefold hollow site in Al_{13}, since the building energy at the bridge site is already large enough to cause H_2 to dissociate.

[28] R. Kawai (private communication).

[29] M. Manninen, J. Mansikka-aho, S. N. Khanna, and P. Jena, Solid State Commun. **85**, 11 (1993).

[30] S. N. Khanna and P. Jena, Chem. Phys. Lett. **219**, 479 (1994).

[31] *Aluminum Alloy: Structure and Properties,* edited by L. F. Mondolfo (Butterworths, London, 1976).